TU Delft

Delft University of Technology

A comparison of data-driven internal multiple elimination strategies and their consequences for imaging

Zhang, L.; Slob, E.

DOI
10.3997/2214-4609.201901518

Publication date
2019

Document Version
Final published version

Published in
81st EAGE Conference and Exhibition 2019

Citation (APA)
Zhang, L., & Slob, E. (2019). A comparison of data-driven internal multiple elimination strategies and their consequences for imaging. In *81st EAGE Conference and Exhibition 2019* Article Th_R04_05 EAGE. https://doi.org/10.3997/2214-4609.201901518

Important note
To cite this publication, please use the final published version (if applicable).
Please check the document version above.

Copyright
Other than for strictly personal use, it is not permitted to download, forward or distribute the text or part of it, without the consent of the author(s) and/or copyright holder(s), unless the work is under an open content license such as Creative Commons.

Takedown policy
Please contact us and provide details if you believe this document breaches copyrights.
We will remove access to the work immediately and investigate your claim.

This work is downloaded from Delft University of Technology.
For technical reasons the number of authors shown on this cover page is limited to a maximum of 10.

Green Open Access added to TU Delft Institutional Repository

'You share, we take care!' – Taverne project

https://www.openaccess.nl/en/you-share-we-take-care

Otherwise as indicated in the copyright section: the publisher is the copyright holder of this work and the author uses the Dutch legislation to make this work public.

2019 EAGE ANNUAL
81ST CONFERENCE + EXHIBITION
LONDON | THE UNITED KINGDOM

Th_R04_05

A Comparison of Data-Driven Internal Multiple Elimination Strategies and Their Consequences for Imaging

L. Zhang[1]*, E. Slob[1]

[1] Delft University of Technology

Summary

We compare two data-driven internal multiple reflection elimination schemes derived from regular Marchenko equations and Inverse Scattering Series (ISS). The scheme derived from regular Marchenko equations creates a new data set without internal multiple reflections. The scheme derived from ISS is equal to the result after the second iteration of the Marchenko-based scheme. It can attenuate internal multiple reflections with residuals. We evaluate the success of two schemes with a 2D complex numerical example. It is shown that Marchenko-based data-driven scheme is relatively more robust for internal multiple reflection elimination.

Introduction

Internal multiple reflections can be very strong and cause artefacts in the migration image from land and marine data. Much effort has been devoted to their removal in data domain and several schemes have been developed. The Inverse Scattering Series (ISS) internal multiple reflection elimination scheme (Weglein et al., 1997) and its derivatives (Ten Kroode, 2002; Löer et al., 2016) are examples. These schemes predict all orders of internal multiple reflections in one step without model information. Adaptive subtraction can be used to subtract the predicted internal multiple reflections from the measured data because of the approximate amplitude of the predicted events. Unfortunately, adaptive subtraction has two major problems. One is that only an overall amplitude correction is carried out. The other is that the primary reflections will also be removed when they overlap with internal multiple reflections.

Van der Neut and Wapenaar (2016) and Zhang and Staring (2018) propose a data-driven internal multiple reflection elimination scheme to account for all orders of internal multiple reflections without adaptive subtraction. It is derived from the regular Marchenko equations (Slob et al., 2014; Wapenaar et al., 2014) and no model information is required. Zhang and Slob (2018) extend the scheme to include the elimination of free-surface multiple reflections. In that scheme free-surface and internal multiple reflections are eliminated successfully in one step without model information or adaptive subtraction. The performance of this scheme in 2D numerical examples has been illustrated, but the validation on field data has not been shown yet.

In this abstract, we compare the data-driven internal multiple reflection elimination schemes derived from regular Marchenko equations (van der Neut and Wapenaar, 2016; Zhang and Staring, 2018) and from ISS (Ten Kroode, 2002; Löer et al., 2016). The comparison covers the theory and performance in a complex numerical example in detail. The abstract is organized as follows. In the theory section, we analyse the difference and relation between the two schemes. In the numerical example section, we test both schemes in a complex numerical example to compare their performance and investigate the consequences for the migration image. Finally, we end with conclusions.

Theory

We indicate time as t and a spatial location as $\mathbf{x}=(\mathbf{x}_{\mathrm{H}},z)$ with $\mathbf{x}_{\mathrm{H}}=(x,y)$, where z denotes depth and $\mathbf{x}_{\mathrm{H}}$ denotes the vector containing the horizontal coordinates. We express the acoustic impulse reflection response as $R(\mathbf{x}_0',\mathbf{x}_0,t)$, where $\mathbf{x}_0'$ denotes the receiver position and $\mathbf{x}_0$ denotes the source position at the surface $\partial\mathbf{D}_0$. The surface $\partial\mathbf{D}_0$ is defined at $z=0$. We assume the medium is lossless.

Marchenko multiple elimination (MME)

The MME scheme is derived from the regular Marchenko equations (Slob et al., 2014; Wapenaar et al., 2014) with the help of projection scheme presented by van der Neut and Wapenaar (2016). The details of the derivation can be found in van der Neut and Wapenaar (2016) and Zhang and Staring (2018). The equation can be given as

$$R_t(\mathbf{x}_0',\mathbf{x}_0'',t)=R(\mathbf{x}_0',\mathbf{x}_0'',t)+[\sum_{m=1}^{\infty}(\mathbf{R}\Theta_\tau^{t-\tau}\mathbf{R}^*\Theta_\tau^{t-\tau})^m R](\mathbf{x}_0',\mathbf{x}_0'',t), \quad (1)$$

where $\mathbf{R}$ indicates a convolution integral operator of the reflection response R with any wave field and $\mathbf{R}^*$ indicates a correlation integral operator. $\Theta_\tau^{t-\tau}$ is the truncation operator to exclude values outside of the window $(\tau,t-\tau)$, τ is a positive value to account for the finite bandwidth of the data, and R_t denotes the retrieved multiple-free primary reflections. The first term in the right-hand side of equation (1) is the original reflection data with internal multiple reflections. Consequently, the second term in the right-hand side of equation (1) can be seen as an operator to eliminate all orders of internal multiple reflections in the original reflection data. The first update of the second term in the right-hand side of equation (1) can be given in the integral form as

$$M_1(\mathbf{x}_0',\mathbf{x}_0'',t) = \int_0^{+\infty} dt' \int_{\partial \mathbf{D}_0} d\mathbf{x}_0''' R(\mathbf{x}_0',\mathbf{x}_0''',t') H(t-t'-\tau) \times \int_0^{+\infty} dt'' \int_{\partial \mathbf{D}_0} d\mathbf{x}_0 R(\mathbf{x}_0''',\mathbf{x}_0,t'') H(t'-t''-\tau) R(\mathbf{x}_0,\mathbf{x}_0'',t-t'+t''). \quad (2)$$

where M_1 indicates the predicted result of the first update and H indicates the Heaviside function to impose the truncation. As discussed by van der Neut and Wapenaar (2016), equation (2) predicts all orders of internal multiple reflections at once with approximate amplitude, and the following updates of the second term in the right-hand side of equation (1) improve the amplitude of internal multiple reflections predicted in the first update.

The scheme uses only the measured reflection responses and a time truncation operator to remove all orders of internal multiple reflections. Therefore, we claim that equation (1) presents a scheme that runs in an automated unsupervised way without model information or adaptive subtraction.

Ten Kroode and Löer internal multiple attenuation (TKL)

The scheme derived from the third term of ISS by Ten Kroode (2002) and Löer et al. (2016) can also predicts all internal multiple reflections. The equation is given by

$$M_{TKL}(\mathbf{x}_0',\mathbf{x}_0'',t) = \int_0^{+\infty} dt' \int_{\partial \mathbf{D}_0} d\mathbf{x}_0''' R(\mathbf{x}_0',\mathbf{x}_0''',t') H(t-t'-\tau) \times \int_0^{+\infty} dt'' \int_{\partial \mathbf{D}_0} d\mathbf{x}_0 R(\mathbf{x}_0''',\mathbf{x}_0,t'') H(t'-t''-\tau) R(\mathbf{x}_0,\mathbf{x}_0'',t-t'+t''), \quad (3)$$

where M_{TKL} indicates the prediction of internal multiple reflections. Note that equation (3) is slightly different from the equation in Löer et al. (2016) because different normalization has been used and ε_1 and ε_2 have been replaced by the half wavelength τ of the source wavelet here. The TKL scheme can be formulized as

$$R'_{TKL}(\mathbf{x}_0',\mathbf{x}_0'',t) = R(\mathbf{x}_0',\mathbf{x}_0'',t) + M_{TKL}(\mathbf{x}_0',\mathbf{x}_0'',t). \quad (4)$$

where R'_{TKL} indicates multiple-attenuated data set.

Equation (3) is exactly the same as equation (2). It means that all internal multiple reflections are predicted with approximate amplitude by equation (3). The retrieved data R'_{TKL} in equation (4) contains primary reflections and residuals of internal multiple reflections. Hence, the TKL scheme is an internal multiple reflection attenuation scheme.

Example

In this section, we apply both schemes to a complex numerical example to test the performance and investigate the consequences for imaging. Figures 1(a) and 1(b) give the velocity and density values of the model. Absorbing boundary conditions are applied around the model. Sources and receivers are positioned at the top surface of the model and the spacing is 10m. A Ricker wavelet with 20Hz centre frequency is emitted by the sources. We have computed the reflection responses for 601 shots and 601 traces per shot, one of the modelled reflection responses is shown in Figure 2(a). Note that the direct wave has been removed from the modelled data. The red arrows in Figure 2(a) indicate some of the internal multiple reflections. We use the modelled reflection responses as inputs to solve equations (1) and (4) for R_t and R'_{TKL}, respectively. The corresponding retrieved data sets are shown in Figures 2(b) and 2(c). It can be seen that internal multiple reflections, which are present in Figure 2(a), have been totally removed and primary reflections well preserved in Figure 2(b). It illustrates the success of MME scheme for internal multiple reflection elimination without model information or adaptive subtraction. The data set shown in Figure 2(c), which is retrieved by the TKL scheme, contains primary reflections and residuals of internal multiple reflections. It illustrates that TKL scheme can reduce the strength of internal multiple reflections. We migrate the modelled and retrieved data sets to image the medium and investigate the consequences for imaging. The correct velocity model is used for the three data sets. The images are obtained using a one-way wave equation migration scheme and

shown in Figures 3(a), 3(b), and 3(c). The image shown in Figure 3(a) is from the modelled reflection responses. It contains artefacts arising from internal multiple reflections. However, the image shown in Figure 3(b), which is from the resulting data set of MME, clearly show the primary reflectors without artefacts due to internal multiple reflections. The image shown in Figure 3(c), which is from the resulting data set of TKL, contains artefacts arising from residuals of internal multiple reflections. Although the artefacts in Figure 3(c) are weaker compared with those in Figure 3(a), they are still strong enough to possibly cause erroneous interpretation.

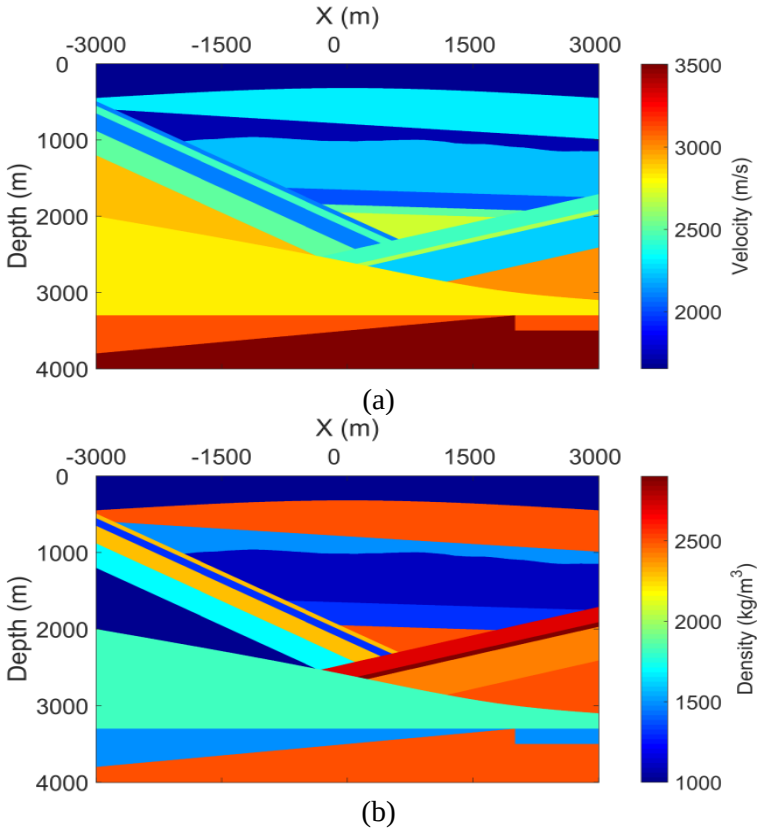

Figure 1 *The (a) velocity and (b) density values of the model.*

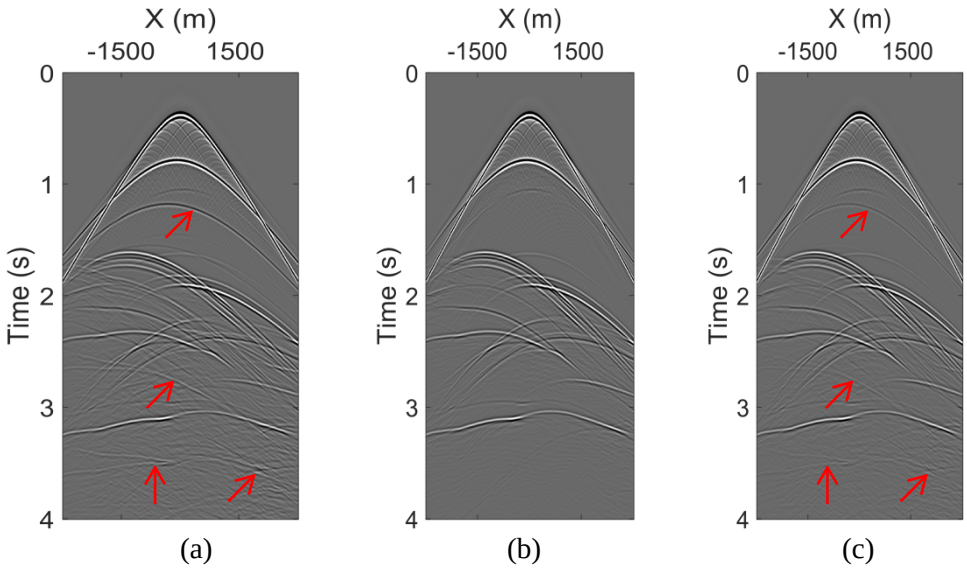

Figure 2 *The (a) modelled reflection response and the (b) retrieved data set by MME and the (c) retrieved data set by TKL. Red arrows in (a) and (c) indicate multiples and residuals.*

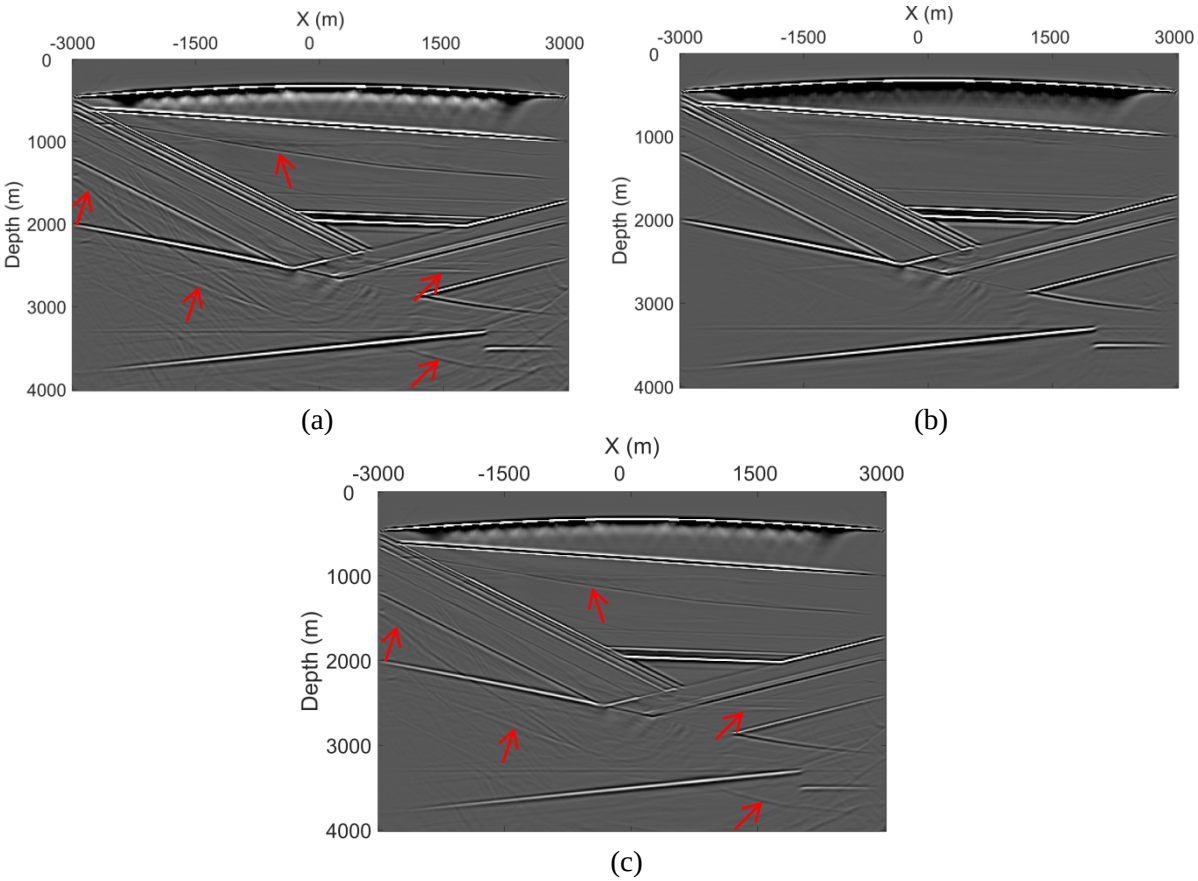

Figure 3 *(a) Image retrieved from the modelled reflection responses and (b) image retrieved from the resulting data set of MME and (c) image retrieved from the resulting data set of TKL. Red arrows in (a) and (c) indicate artefacts due to internal multiple reflections and residuals.*

Conclusions

We have compared two data-driven internal multiple elimination schemes from theory to performance in a numerical example. MME is derived from Marchenko equations and TKL from ISS. The relation between the two schemes is analysed, showing that the TKL scheme is equal to carrying out one iteration of the MME scheme. The numerical example shows that the MME scheme has an excellent performance in removing internal multiple reflections and that the TKL scheme attenuates the internal multiple reflections but leaves residuals. These residuals can cause artefacts in the migration image.

References

Löer, K., Curtis, A. and Meles, G.A. [2016] Relating source-receiver interferometry to an inverse-scattering series to derive a new method to estimate internal multiples. *Geophysics*, 81, Q27–Q40.
Slob, E., Wapenaar, K., Broggini, F. and Snieder, R. [2014] Seismic reflector imaging using internal multiples with Marchenko-type equations. *Geophysics*, 79, S63–S76.
Ten Kroode, P.E. [2002] Prediction of internal multiples. *Wave Motion*, 35, 315–338.
van der Neut, J. and Wapenaar, K. [2016] Adaptive overburden elimination with the multidimensional Marchenko equation. *Geophysics*, 81, T265–T284.
Wapenaar, K., Thorbecke, J., van der Neut, J., Broggini, F., Slob, E. and Snieder, R. [2014] Marchenko imaging. *Geophysics*, 79, WA39– WA57.
Weglein, A.B., Gasparotto, F.A., Carvalho, P.M. and Stolt, R.H. [1997] An inverse scattering series method for attenuating multiples in seismic reflection data. *Geophysics*, 62, 1975–1989.
Zhang, L. and Staring, M. [2018] Marchenko scheme based internal multiple reflection elimination in acoustic wavefield. *Journal of Applied Geophysics*, 159, 429-433.
Zhang, L. and Slob, E. [2019] Free-surface and internal multiple elimination in one step without adaptive subtraction. *Geophysics*, 84(1), A7– A11.